

Design and implementation of jerk-controlled elevator systems using S-curve motion profiles

Ali Abdulkareem Ali¹, Fatma Ben Salem^{1,2}, Jamal A.-K. Mohammed³

¹Control and Energy Management Laboratory, Sfax Engineering School, University of Sfax, Sfax, Tunisia

²Prince Sattam Bin Abdulaziz University, College of Engineering, Department of Electrical Engineering, Alkharj, Saudi Arabia

³Electromechanical Engineering Department, University of Technology, Baghdad, Iraq

Article Info

Article history:

Received Aug 25, 2024

Revised Jan 28, 2025

Accepted Mar 1, 2025

Keywords:

Elevator

Induction motor

Jerk

S-curve

Sensorless vector control

Variable frequency drive

ABSTRACT

Electric elevators often experience significant jerks that can shorten their lifespan and cause passenger discomfort, especially during acceleration and deceleration. To address this issue, this study presents the development and implementation of S-curve motion profiles for a prototype three-floor rope elevator system. The elevator cabin is driven by a three-phase induction motor using sensorless vector control technology, with a variable frequency drive (VFD) managing the cabin's velocity. The findings indicate that employing S-curve motion profiles reduces jerk by approximately 29.43% when the elevator is ascending without a load and by 48.15% when descending without a load. In the loaded scenario, the elevator experiences a significant reduction in jerk, decreasing by 48.78% during ascent and 52.08% during descent. By smoothing out abrupt acceleration changes, the reduction in jerk leads to a more seamless motion of the elevator car, significantly enhancing passenger comfort. Consequently, this approach improves the efficiency and reliability of elevator operations, providing a versatile platform for future vertical transportation advancements.

This is an open access article under the [CC BY-SA](https://creativecommons.org/licenses/by-sa/4.0/) license.



Corresponding Author:

Ali Abdulkareem Ali

Control and Energy Management Laboratory, Sfax Engineering School, University of Sfax

Sfax, Tunisia

Email: ali-abulkareem.ali@enis.tn

1. INTRODUCTION

Advancements in electromechanical technologies, especially lifts, have greatly accelerated the speed of urban construction. With the increasing vertical expansion of cities, the demand for effective vertical transit systems has become crucial in multi-story buildings. Elevators not only meet this requirement but also cater to the needs of contemporary industrial expansion.

Any multi-story commercial building must have elevators to ensure the smooth movement of people and products. It is interesting to comprehend the diverse kinds of elevator systems and their distinct features. The most common types of elevator systems are traction elevators [1]-[3], hydraulic elevators [4]-[6], machine room-less (MRL) elevators [7]-[9], pneumatic elevators [10]-[12], and freight elevators [13]-[15].

On the other hand, the elevator can be classified according to the driving method into AC drive elevator [16], [17], DC drive elevator [18], [19], hydraulic elevator [4], rack and pinion elevator [20], [21], screw elevator [22], [23], and linear motor-driven elevator [24], [25]. The most prevalent kind of elevator technology is the traction elevator. The elevator cabin is raised and lowered using a counterweight, a system of belts, and cables (wire rope). Although they are very dependable and provide a smooth ride, traction elevators need a separate machine room, which can take up valuable space in the building structure.

Passenger well-being, especially in high-speed elevators in skyscrapers, is a crucial consideration [26], [27]. These elevators usually suffer from complications such as ripple forces (or jerks) during their operation and movement within building structures. The exertion of these forces can generate powerful jolts that not only cause discomfort to passengers but also have the potential to damage the mechanical and electrical components of the elevator, thereby diminishing the overall lifespan of the lifting system. Managing these sudden movements is crucial for minimizing their impact and enhancing passenger comfort. High-performance control methods, such as variable frequency drives (VFDs), are among the most effective solutions. The VFD controls the velocity and rotational force of AC motors by adjusting the input voltage and frequency. The main goal of elevators is to maintain a constant ratio of voltage to frequency (V/f) [16]. This feature is essential for minimizing mechanical stress, increasing system durability, and guaranteeing a smooth start and stop of elevator operation.

Numerous methods have been proposed to address the problem of sudden movements during elevator floor transitions, which have been extensively examined. An inventive drive method was proposed by Das *et al.* [19] for mid-rise and mid-speed elevators. A permanent magnet DC motor with PID control powered the cabin. There were several benefits to using this motor, including as improved riding comfort, less jerk, and enhanced efficiency.

Shreelakshmi and Agarwal [28] proposed combining rectangular and sinusoidal jerk patterns to create a smooth speed profile that enhances comfort while maintaining travel time. Crăciun *et al.* [29] conducted a comparative study on changes in the elevator's kinematic parameters using electronic velocity modeling in MATLAB. The study focused on achieving smooth deceleration by applying S-curves. Masoudi [30] suggested employing a linear switching reluctance motor (LSRM) in an elevator system with an appropriate speed pattern for optimal and smooth travel with minimal jerk. DTC in induction motor drivers was extensively studied by Arafa *et al.* [31] utilizing the space vector modulated-direct torque control (SVM-DTC) approach. Speed profiling could increase elevator comfort.

Shreelakshmi and Agarwal [32] developed a loss minimization method for induction motor-driven elevators. This is needed to find an energy-optimal velocity pattern. The goal function is a differential equation that ties motor power losses to rotor speed. Speed and acceleration are limited by passenger comfort. Pontryagin's minimum principle finds the best trajectory by choosing a Hamiltonian function.

The permanent magnet synchronous motor (PMSM) responds quickly to changes, but the elevator speed controller's limited bandwidth can cause issues. When rotor flux linkage or static friction deviates from set values, traditional jerk control methods may lead to higher starting energy. To mitigate these problems, Rangarajan *et al.* [33] proposed a novel disturbance observer that temporarily modifies the stator flux linkage speed rather than the torque/current during starting.

Qiu *et al.* [27] proposed a strategy to improve vibration-related high-speed elevator design. They also demonstrated how the key parameters affected the high-speed elevator horizontal vibration system and chose the optimum way to improve these elevators' horizontal vibration performance, operational stability, and ride comfort. Onat *et al.* [25] used a permanent magnetic synchronous linear motor fed from a VFD and programmed in the best V/f pattern for the best speed curve profile to control the elevator cab's speed so it started and stopped smoothly and traveled consistently across the elevator floors with minimal jerk. This driver cut jerk values by 88% compared to the standard scenario.

There are several limitations to the current research on elevator systems, even if there have been great advances. Power logic controllers (PLCs) are the backbone of many older control systems, but they might not have the processing power to support more complex control algorithms. Furthermore, conventional systems frequently make use of uncomplicated switching or transistor modules based on relays, which do not have integrated protection or accurate feedback mechanisms. The necessity for thorough real-time monitoring and modifications has not been sufficiently addressed in the research that has investigated PID-controlled DC motors or sinusoidal jerk patterns. In addition, many studies underutilize S-curve profiles, often resulting in insufficient jerk reduction and suboptimal ride comfort. To enhance elevator performance and passenger comfort, more advanced and integrated control methods are necessary, as these limits have shown.

This research proposes a sensorless vector control (SVC)-based three-floor roping elevator prototype with an optimized S-curve speed profile operated by a three-phase induction motor. VFD regulates motor speed. The VFD is fully integrated with an STM32 microcontroller's exact control. This research uses the INVT GD20 VFD to improve motor performance and speed regulation. Complex control systems including infrared sensors and limit switches have been built into the elevator. The optimal S-curve velocity profile design and implementation will be the focus of this study. The S-curve approach reduces mechanical jerks by eliminating sudden acceleration and deceleration changes, unlike linear profiles. The sinusoidal limited-jerk trajectory approach described by Mutlu [34], initially applied to PMSM, is well-suited for elevator systems. In this study, the approach is adapted for use with an induction motor (IM), demonstrating its effectiveness in achieving time optimization and smooth jerk transition in the IM-driven elevator system. The suggested elevator technology, which mimics three-story elevators, requires this.

The study has some objectives: i) Enhancing passenger comfort through minimized mechanical jerks under unloaded and loaded conditions; ii) Improving the efficiency and reliability of the elevator system by taking advantage of advanced motor speed control and microcontroller integration; and iii) Building an efficient elevator model that mimics a real-world elevator and is scalable for future elevator systems, providing a framework for implementing similar technologies in commercial vertical transportation solutions.

2. THEORETICAL BASIS AND PROPOSED METHOD

2.1. Induction motor (IM)

In a reference frame that rotates in synchronization, Figure 1 depicts the d-q equivalent circuit of a three-phase induction motor [35], [36]. Figure 1 displays the d-q circuit that fulfills conditions (1) to (5). These equations [35], [36] provide the standard dynamic model of an induction motor, without considering magnetic material saturation, rotor resistance changes due to skin effect, and stator resistance fluctuations due to temperature variations.

$$v_{qr} = R_r i_{qr} + \frac{d}{dt} \Psi_{qr} + (\omega_e - \omega_r) \Psi_{qr} \quad (1)$$

$$v_{dr} = R_r i_{dr} + \frac{d}{dt} \Psi_{dr} + (\omega_e - \omega_r) \Psi_{dr} \quad (2)$$

$$\Psi_{qr} = L_{lr} i_{qr} + L_m + (i_{qs} + i_{qr}) \quad (3)$$

$$\Psi_{dr} = L_{lr} i_{dr} + L_m + (i_{ds} + i_{dr}) \quad (4)$$

$$T_e = \frac{3 P L_m}{2 \times 2 L_r} (\phi_{dr} i_{qs} - \phi_{qr} i_{ds}) \quad (5)$$

Where the variables v_{qr} and v_{dr} denote the rotor voltages in d-q coordinates, whereas, i_{qr} , i_{dr} , Ψ_{qr} , and Ψ_{dr} indicate the currents and fluxes in d-q coordinates, ω_e is the revolving magnetic field angular speed, ω_r symbolizes the slip angular speed, while T_e represents the electromagnetic torque. The parameters of the motor are specified as follows: P denotes the poles' number, R_r represents the rotor resistance, L_m represents the motor mutual inductance, and L_r represents the rotor inductance. In the induction motor model, R_r affects the heat losses and torque production in the motor. A higher R_r can lead to increased losses and reduced efficiency. The mutual inductance, L_m characterizes the coupling between the stator and rotor magnetic fields, influencing the motor's ability to produce torque.

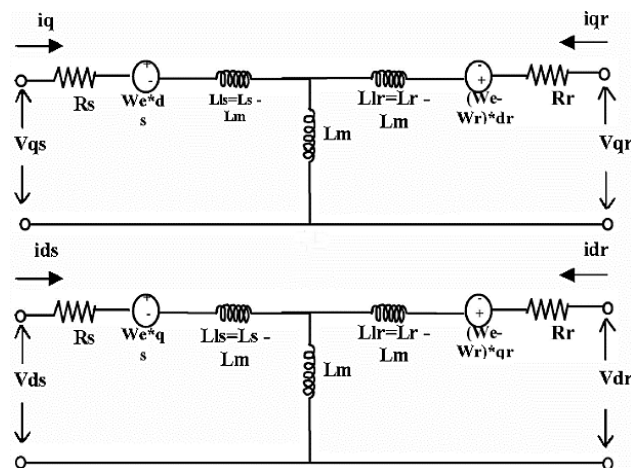


Figure 1. d-q equivalent circuit of induction motor

The motor's electromagnetic torque T_e is generated due to the interaction between the stator's magnetic field and the rotor currents. Variations in the slip angular speed ω_r directly affect the torque production, which is crucial for controlling the elevator's movement. Controlling the torque and slip of the induction motor plays a crucial role in reducing jerk during elevator motion. Sensorless vector control is a technique used to manage the motor's torque and speed precisely without relying on physical sensors. This

approach simplifies the system while still providing accurate control, enabling smoother acceleration and deceleration, which helps to minimize abrupt changes in motion (jerk).

2.2. Variable frequency drive (VFD)

VFD operates by adjusting input voltage and frequency, adjusting the torque and speed of AC motors and is widely used for industrial applications. In recent years, the trend of utilizing VFD technology and speed control in the current motors has gained traction. Recent innovations in magnetic materials and power electronics have played a large role in the mass adoption of VFDs. VFDs must fulfil certain requirements in elevator systems, such as smooth starts and stops, comfortable rides, accurate floor leveling, and effective braking [16], [37].

The speed of the AC motor (n) is determined by the number of its poles (p) and the input frequency (f) according to (6).

$$n_r = \frac{(1-s)120f}{p} \quad (6)$$

Where s is the motor slip. Modifying the frequency applied to a motor can be a simple and effective way to regulate its speed.

The VFD controls the induction motor's speed by varying the input frequency, which, along with the number of poles p determines the motor's synchronous speed. The slip, defined as the difference between synchronous speed and rotor speed, influences the torque generated. Proper control of slip allows for smooth acceleration and deceleration, minimizing jerk during elevator operation. Additionally, implementing an S-curve profile further enhances this process by flattening acceleration transitions, reducing abrupt changes in speed, and improving overall ride comfort.

2.3. Sensorless vector control (SVC)

This is an advanced method of controlling the torque and speed of AC motors, normally referred to as field-oriented control (FOC), which is typically used for traction applications for elevators. For example, elevators utilize precise control systems for their motors. Motors can feed back their rotor position and speed to determine the active control performance, but FOC performs much better without resorting to these physical sensors. This approach applies mathematical models and estimates derived from the electrical readings of the engine, like voltage and current.

This method simplified the system and minimized maintenance requirements while ensuring accurate, quick control by dividing the motor current into two parts: one producing flux and the other producing torque. This decoupling allows for independent control of motor torque and flux, similar to controlling a DC motor, but applied to AC motors [37]. Figure 2 illustrates the block diagram of the sensorless vector control system for an induction motor (IM). In this setup, the rotor speed and flux are estimated without using physical sensors, allowing the system to accurately control motor speed and torque. The control strategy involves converting the motor's three-phase currents and voltages into a rotating reference frame (dq frame) for easier control.

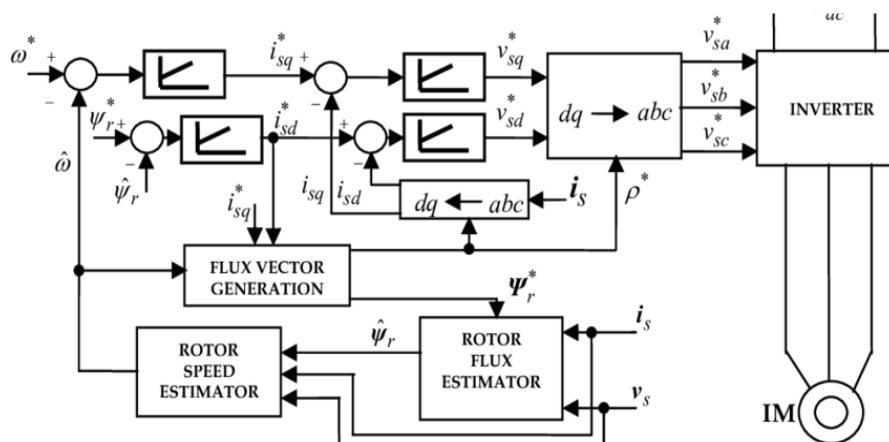


Figure 2. Sensorless vector-controlled induction motor drive

2.4. Jerk reduction in elevators

The most common elevator motion profiles are triangular and trapezoidal. In Figure 3(a), the system speed increases from zero to its maximum value, sustains it for a predetermined duration (or distance), and then decelerates to zero in a trapezoidal motion profile. However, the triangle motion profile accelerates to its maximum speed, then decelerates instantly to zero, maintaining a constant velocity. Unfortunately, none of these move profiles are appropriate for motion systems, especially elevators that must travel smoothly, position properly, and remain stable after the move. Acceleration or deceleration causes jerks.

Similar to velocity, jerk is acceleration's rate of change. Jerk's acceleration rate is its increase or decrease. Jerk gives fast, jerky action, making it uncomfortable. An abrupt acceleration change, or jerk, shakes industrial systems. Higher jerks cause more vibrations. Vibrations slow the settling but diminish positioning accuracy.

Avoiding jerks is best done by slowing down. The "jerky" trapezoidal motion profile can be replaced by an S-curve motion profile in motion control systems [25], [38], [39]. An infinite jerk and rapid acceleration characterize a trapezoidal motion profile. To reduce jerk, acceleration and deceleration transitions are flattened into an "S" form.

Figure 3(b) shows a trapezoidal and triangular motion's acceleration profile as a step function, with acceleration rapidly growing to its maximum and deceleration instantaneously reducing to zero. A major jolt will harm passengers and the elevator's mechanical system. When a motion follows an S-curve, the acceleration profile is trapezoidal, and acceleration and slowing are moderate.

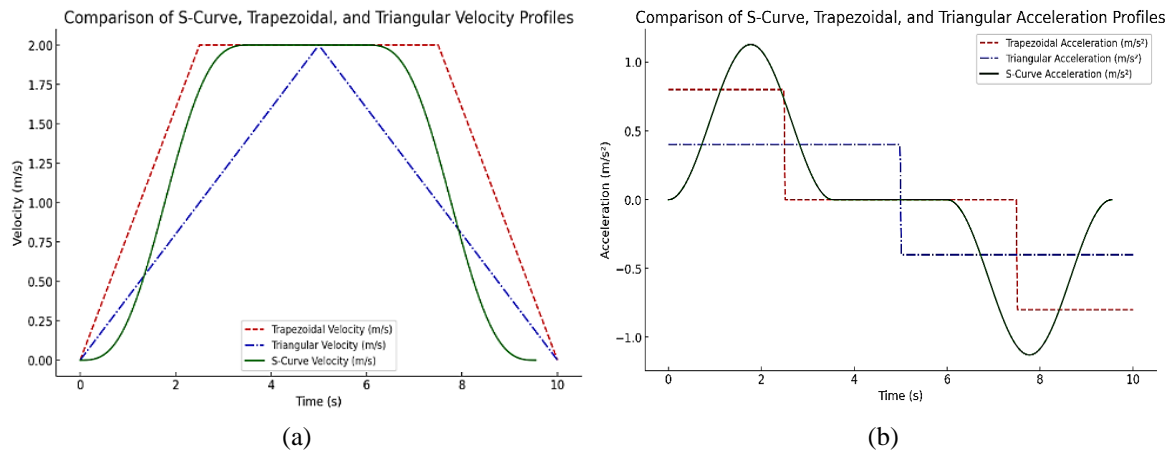


Figure 3. Comparison of triangular, trapezoidal, and s-curve profiles: (a) velocity and (b) acceleration

For the elevator system to provide a smooth electro-mechanical torque that lowers vibration and lengthens lifespan, the acceleration must have a continual and smooth waveform. Choosing the best form for the jerk change is necessary to produce smooth acceleration. This study improves the sinusoidal limited-jerk trajectory method to better suit elevator operation, providing a solution that optimizes both time efficiency and smooth motion. A limited jerk for the intended motion is guaranteed when a sinusoidal jerk waveform is used, as specified by (7).

$$j = \begin{cases} j_m \sin \frac{2\pi}{T} t, & t \in [0, T] \\ 0, & t \in [T, t_2] \\ -j_m \sin \frac{2\pi}{T} (t - t_2), & t \in [t_2, t_3] \end{cases} \quad (7)$$

Where t_3 is the overall period of cabin movement, the time T is taken for acceleration or deceleration, t_2 is equal to $t_3 - T$, which is the instant when the cabin begins deceleration, and j_m is the maximum jerk amplitude.

The following relationships, based on (7), express the acceleration a , velocity v , and displacement d in specified intervals, as in (8)-(10).

$$a = \int j \, dt + C_a \quad (8)$$

$$v = \int a \, dt + C_v \quad (9)$$

$$d = \int v \, dt + C_d \quad (10)$$

Constants C_a , C_v , and C_d are determined from initial conditions. Acceleration is calculated from the expression for jerk, as in (11).

$$a = \cos\left(\frac{2\pi}{T}t\right) + C_a \quad (11)$$

C_a is calculated based on the premise that the acceleration is zero at $t = 0$, given in (12).

$$C_a = \frac{j_m T}{2\pi} \quad (12)$$

During the interval $t \in [0, T]$, the acceleration expression is as in (13).

$$a = \frac{j_m T}{2\pi} \left(1 - \cos\left(\frac{2\pi}{T}t\right)\right) \quad (13)$$

Constants for all other values are derived similarly, resulting in equations for acceleration, velocity, and displacement (Figure 4).

$$a = \begin{cases} \frac{j_m T \left(1 - \cos\left(\frac{2\pi}{T}t\right)\right)}{2\pi}, \\ a_m, \\ -\frac{j_m T \left(1 + \cos\left(\frac{2\pi}{T}(t_2 - t)\right)\right)}{2\pi} \end{cases} \quad (14)$$

The acceleration equation describes the rate of change of velocity with respect to time. By controlling the acceleration using the S-curve profile, the transition between different velocity levels is made smoother, thereby reducing abrupt changes in acceleration (jerk). This contributes to a more comfortable ride.

$$v = \begin{cases} \frac{j_m T \left(2\pi t - T \sin\left(\frac{2\pi}{T}t\right)\right)}{4\pi^2}, \\ \frac{j_m T^2}{2\pi}, \\ \frac{j_m T}{2\pi} \left(T - \frac{T \sin\left(\frac{2\pi}{T}(t_2 - t)\right) + 2\pi(t - t_2)}{2\pi}\right) \end{cases} \quad (15)$$

$$d = \begin{cases} \frac{j_m T}{4\pi} \left(t^2 - \frac{T^2 \left(1 - \cos\left(\frac{2\pi}{T}t\right)\right)}{2\pi^2}\right), & t \in [0, T] \\ \frac{j_m T^2}{4\pi} (2t - T), & t \in [T, t_2] \\ \frac{j_m T^2}{4\pi} \left[(2t - T) - \frac{(t - t_2)^2}{T} + \frac{T}{2\pi^2} \left[1 - \cos\frac{2\pi}{T}(t - t_2)\right]\right] & t \in [t_2, t_3] \end{cases} \quad (16)$$

The maximum value of displacement can be calculated from (16) at time $t = t_3$ as (17).

$$d_m = j_m \frac{T^2}{2\pi} t_2 \quad (17)$$

By following the given technique, v can be obtained in the steady state, which is referred to as the maximum value of speed, denoted as v_m . By using the expression for velocity magnitude, the interval T can be determined as (18).

$$T = \sqrt{\frac{2\pi v_m}{j_m}} \quad (18)$$

For a given d_m , the time t_2 can be determined from (17). A list of symbols for all equations has been included in Table 1.

The use of the S-curve profile allows for gradual changes in acceleration, which prevents sudden spikes in jerk, as depicted in the Figure 4, illustrates how the S-curve provides a smooth progression for displacement, velocity, acceleration, and jerk over time. This smooth transition minimizes the impact on passengers, enhancing ride comfort. The S-curve's ability to gradually increase and decrease acceleration not only improves comfort but also reduces mechanical stress on the elevator components, leading to lower maintenance needs and extending the lifespan of the system. This makes the S-curve profile especially suitable for passenger elevators where comfort and durability are priorities.

The implementation of the S-curve profile and sensorless vector control involves several key steps. It starts with system initialization, followed by estimating the rotor speed and position using sensorless vector control. The S-curve profile is used to produce reference acceleration commands that facilitate smooth transitions. The commands are parameters to the control system that change the motor torque and speed; being an adaptive system, the computer continues to monitor feedback so that the control system always applies precise commands to the elevator. This is followed by a smooth deceleration at the end that stops the elevator softly for a better ride comfort.

Table 1. A list of symbols for all equations

Symbols	Description	Units	Symbols	Description	Units
j_m	Maximum jerk	m/s^3	d_m	Maximum displacement	m
v_m	Maximum velocity	m/s	t_2	Deceleration moment	Sec
C_a	Acceleration constants	m/s^2	t_3	Total duration of movement	Sec
C_v	Velocity constants	m/s	T	Acceleration/deceleration time	Sec
C_d	Displacement constants	m			

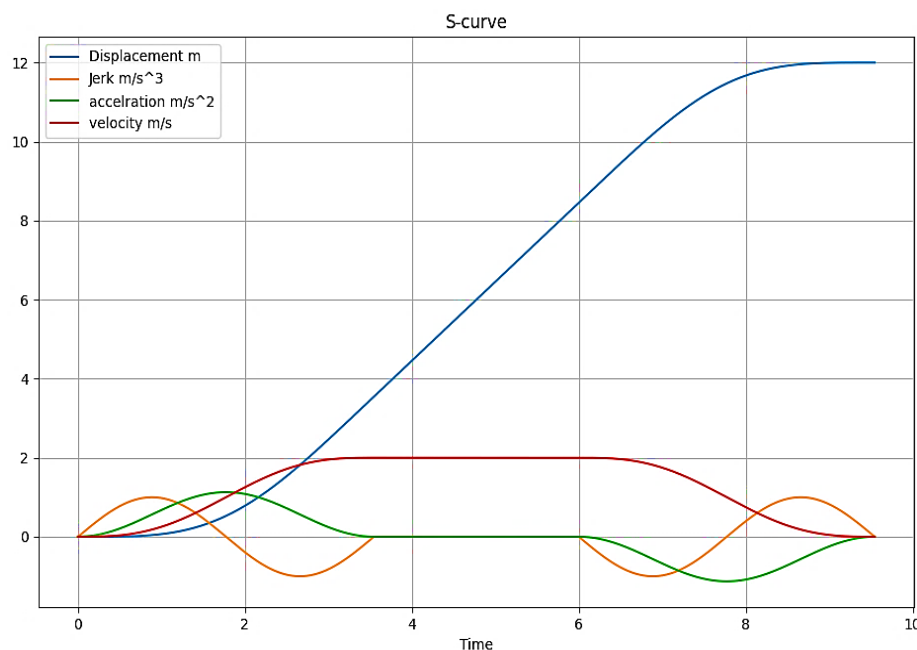


Figure 4. S-curve profiles

3. METHOD

3.1 System construction

The structure of the elevator system prototype is built of iron and consists of three floors, 200 cm high, 45 cm wide, and 55 cm deep. The elevator cab, made of aluminum, has dimensions of 19×30 cm and operates using two pulleys, each with a diameter of 7 cm, which ensures balanced and smooth vertical movement. The cabin is designed to handle a total capacity of approximately 23.3 kg, including its weight.

A 0.75 kW, 1395 rpm, 50 Hz, delta-connected three-phase induction motor located at the top of the structure is chosen to drive the cabin. The motor's torque is effectively transmitted through the pulleys, providing the necessary lifting force to transport the cabin and load efficiently across the floors. The motor provides a rated torque of 8 N.m and operates at a power factor ($\cos \phi$) of 0.75 and line current of 2 A. The motor is also equipped with a brake mechanism to ensure quick and safe stopping.

The motor is controlled by an INVT GD20 VFD. The VFD is a series of variable frequency drives manufactured by INVT, a well-known company that specializes in industrial automation technology, which employs sensorless vector control and an S-curve profile for smooth motion. The VFD is interfaced with the STM32F407VET6 microcontroller, which is a powerful solution for industrial, consumer, and IoT applications.

Three transistor circuits that handle the forward, reverse, and stop signals, which are used to control the motor. Both forward and reverse signals are normally open (NO) contacts, while the stop signal is a normally closed (NC) contact, which becomes open to stop the motor when needed. The elevator has two limit switches (LXW5-11G1) at the top and bottom to stop the cabin over-travel and ensure safe operation, while the elevator cab can be stopped on each floor using infrared sensors, as these sensors generate digital signals when they detect the elevator cabin within their detection range. These signals are processed by an STM32F407VET6 microcontroller, which precisely regulates the elevator's progress to guarantee that it stops at the intended floor.

Figure 5 depicts the experimental setup of the elevator system prototype, highlighting the integration of key components. The flowchart as shown in Figure 6, illustrates the sequence of operations for the elevator system, from floor call handling to motion execution. The process starts with reading the current floor, followed by a check to see if the requested floor is different. If needed, the control system signals the VFD to move the elevator up or down using an S-curve profile for smooth acceleration and deceleration.

During motion, the MPU6050 sensor monitors the elevator's dynamics, sending data for analysis. As the elevator approaches the target floor, sensors detect its position, and the VFD is signaled to stop. The flowchart also accounts for emergency stop handling, ensuring safety by immediately halting the elevator if needed.

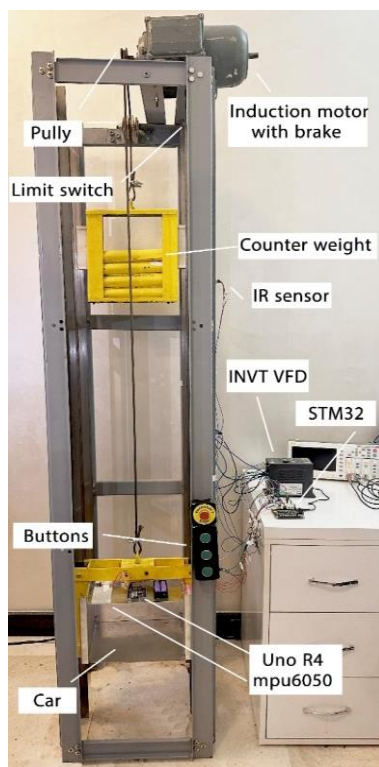


Figure 5. Experimental setup of elevator system prototype

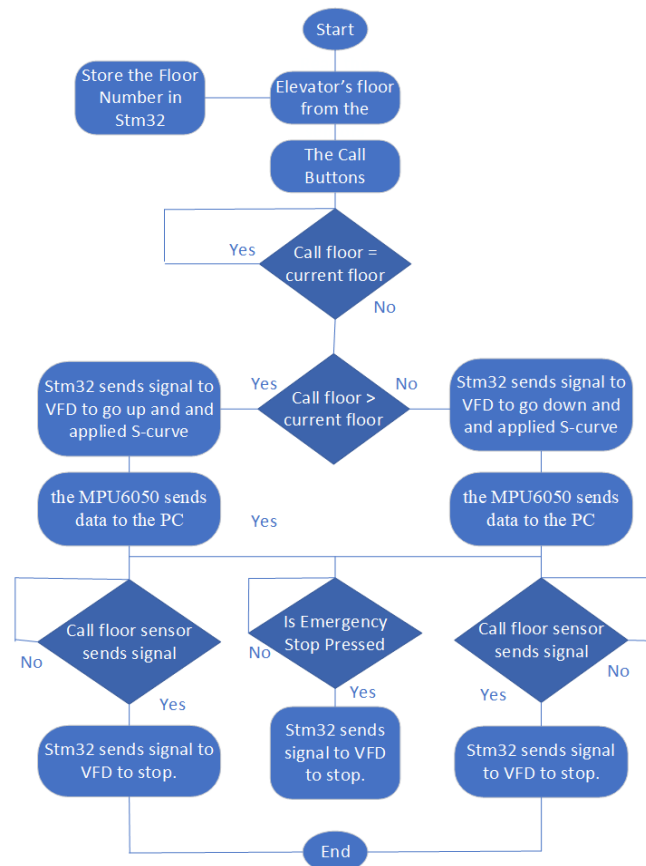


Figure 6. Elevator control process

3.2. Scalability and real-world applications

While the current experimental setup is based on a small-scale prototype, the principles and control strategies developed can be directly applied to full-scale elevator systems in larger buildings. The following factors demonstrate the scalability of the results.

- i) Control strategy adaptation
 - The S-curve motion profile and jerk minimization techniques used in the prototype can be scaled for larger elevators by adjusting parameters such as acceleration, deceleration, and velocity limits to match the requirements of full-size systems. These adjustments ensure the comfort benefits observed in the prototype are maintained.
- ii) Sensor integration and data handling
 - Full-scale implementations can use more advanced sensors for precise motion control and data acquisition. The scalability of sensor technology, such as accelerometers and encoders, allows for similar data collection methods to be used with larger elevators, ensuring accurate control.
- iii) Variable frequency drive (VFD) scaling
 - The VFD used in the prototype can be scaled to handle the power and torque requirements of larger elevator motors. The control algorithms remain the same, but power ratings and hardware configurations would be adapted for the larger system.
- iv) Challenges and adaptations
 - Structural considerations: Full-scale elevators in taller buildings may require additional structural support to minimize vibrations and resonances. The control algorithm may also need to account for variations in load distribution and cable dynamics.
 - Safety standards and regulations: Larger elevators must meet stringent safety standards, which may necessitate additional safety features like emergency braking systems and redundant control mechanisms. The S-curve profile can be integrated into these systems for smoother emergency stops.
 - Power requirements: Scaling up may involve higher power requirements and more complex electrical systems. Efficient power management and control tuning will be essential for maintaining ride quality.

The scalability considerations suggest that the proposed methods can enhance ride comfort and system efficiency in real-life elevator applications, especially in high-rise buildings where jerk reduction is crucial for passenger comfort.

4. RESULTS AND DISCUSSION

The jerk data analysis for the elevator prototype showed a noticeable difference in the no-load and the loaded condition between the case without and with the S-curve motion profile. It is important to analyze the jerk profile with no load (empty car). Used for comparison, baseline, control system validation and areas of improvement. This allows us to lower the high jerk values using the S-curve profiles, so that the drive becomes smoother and ride more comfortable. This foundational analysis sets the stage for further testing with loads, ultimately leading to a comprehensive understanding of the elevator's performance under all load conditions.

4.1. Methodology for calculating jerk

Accurate jerk computation is essential to identify sudden changes in elevator movement that may compromise passenger comfort and safety. The steps for calculating the jerk are as follows:

- The practical procedures include, i) measuring the initial and final accelerations (a_1 , a_2) at the corresponding times t_1 and t_2 and ii) calculating the change in acceleration: $\Delta a = a_2 - a_1$ and the corresponding change in time $\Delta t = t_2 - t_1$. Where Δa is the change in acceleration and Δt is the change in time. The acceleration value (a) has been measured using an MPU6050 accelerometer sensor.
- The jerk (j) is calculated from (19).

$$j = \frac{\Delta a}{\Delta t} \quad (19)$$

Integration of the MPU6050 sensor with the aid of the Arduino Uno R4 Wi-Fi microcontroller makes it easy to analyze the elevator movement. The Uno R4 is an adaptable board that incorporates new enhancements and wireless capabilities with the ease of use of the classic Arduino. It is therefore the ideal option for applications involving distant sensing. The motion-tracking gadget, the MPU6050, combines a three-axis accelerometer and a three-axis gyroscope. For the gyroscope, the sensitivity ranges are ± 250 to ± 2000 dps, and for the accelerometer, they are ± 2 to ± 16 g. The system setup allows for real-time monitoring and analysis of the elevator's motion, with data being sent wirelessly via Wi-Fi network to a remote system for further processing or display, and ensures that the system remains powered independently of the elevator's main power supply, making it highly practical for use in dynamic environments.

4.2. Jerk analysis without S-curve

In the first case (without S-curve, no-load) shown in Figures 7 and 8, the jerk data exhibited significant variability, with sharp peaks and troughs during both upward and downward movement. The maximum positive

jerk value reached approximately 3.33 m/s^3 when going up and 3.24 m/s^3 when going down, while the minimum (most negative) jerk values were around -3.66 m/s^3 and -4.36 m/s^3 , respectively. Such abrupt acceleration changes can cause passenger discomfort and increase mechanical stress on elevator components.

In the second case (without S-curve, with load) shown in Figures 9 and 10, the jerk values remained high, indicating noticeable peaks and troughs similar to the no-load condition. Above, the maximum positive jerk was about 2.87 m/s^3 and the minimum jerk was -3.56 m/s^3 . When downward, the maximum positive jerk was 3.07 m/s^3 , and the minimum jerk was -3.16 m/s^3 . Adding a load slightly altered the jerk patterns but did not significantly reduce the abrupt changes, still posing risks of discomfort and mechanical stress.

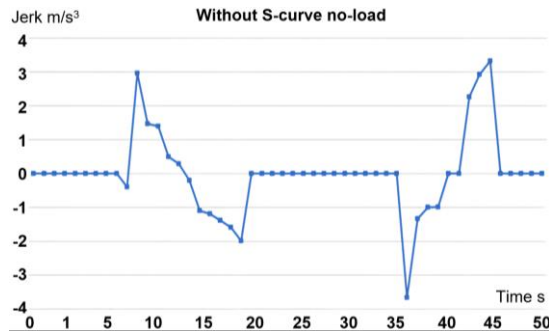


Figure 7. Jerk in 1st case
(without s-curve, no-load, upward)



Figure 8. Jerk in 1st case
(without s-curve, no-load, downward)

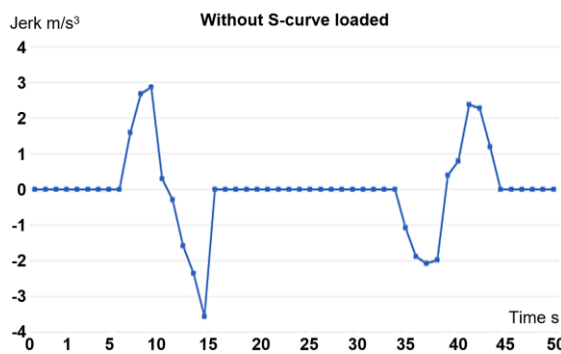


Figure 9. Jerk in the 2nd case
(without s-curve, loaded, upward)

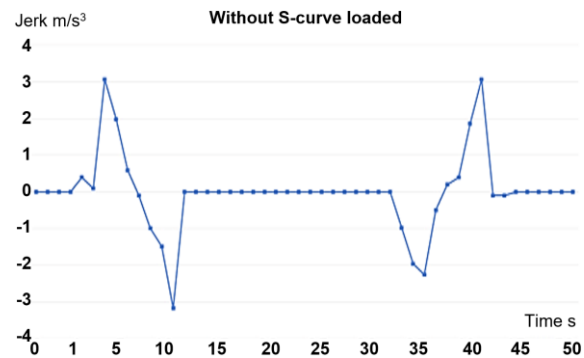


Figure 10. Jerk in the 2nd case
(without s-curve, loaded, downward)

4.3. Jerk analysis with S-curve

In the third case (with S-curve, no load) illustrated in Figures 11 and 12, the transitions were much smoother with fewer abrupt changes. When upward, the maximum positive jerk reduced to approximately 2.35 m/s^3 and the minimum jerk to -2.57 m/s^3 . When downward, the maximum positive jerk is further reduced to about 1.68 m/s^3 , and the minimum jerk to -2.87 m/s^3 .

In the fourth case (with S-curve, with load) shown in Figures 13 and 14, the S-curve profile further smoothed the transitions, providing the most significant improvements. When upward, the maximum positive jerk was about 1.47 m/s^3 and the minimum jerk was -1.37 m/s^3 . Similarly, when downward, the maximum positive jerk remained at 1.47 m/s^3 and the minimum jerk at -1.37 m/s^3 . The S-curve effectively mitigated the impact of the added load, ensuring smoother transitions and enhancing passenger comfort.

Experimental tests under partial load conditions showed that increased load significantly reduced jerk. This is due to the added inertia from greater mass, which dampens abrupt acceleration, creating smoother transitions. While these findings support the S-curve's effectiveness under varied loads, they were excluded from the main analysis for conciseness. Future research could perform a broader analysis across different loads for deeper insights.

4.4. Comparison of control methods

To clarify the differences between various elevator motion control methods, Table 2 compares the S-curve motion profile with alternative approaches such as trapezoidal, triangular profiles, and PID control.

The table highlights key features, including jerk minimization, ride comfort, acceleration smoothness, ease of implementation, and control complexity. The comparison demonstrates that the S-curve profile provides superior jerk minimization and ride comfort due to its smooth acceleration and deceleration transitions. Although it requires more complex calculations, it is ideal for passenger elevators where comfort is a priority. In contrast, trapezoidal and triangular profiles are simpler to implement but lead to more abrupt motion changes, which may reduce ride quality.



Figure 11. Jerk in the 3rd case (with s-curve, no load, upward)

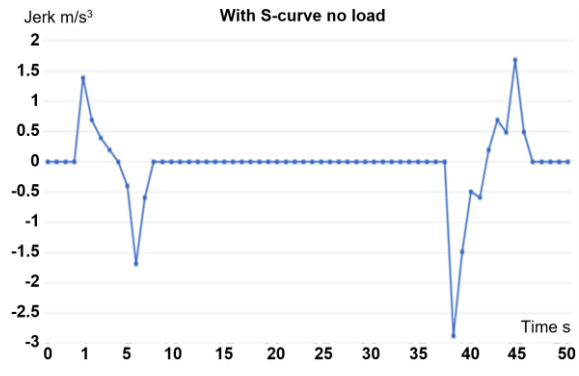


Figure 12. Jerk in the 3rd case (with s-curve, no load, downward)

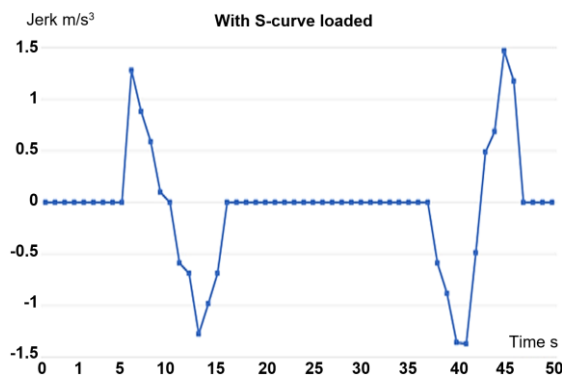


Figure 13. Jerk in the 4th case (with s-curve, loaded, upward)

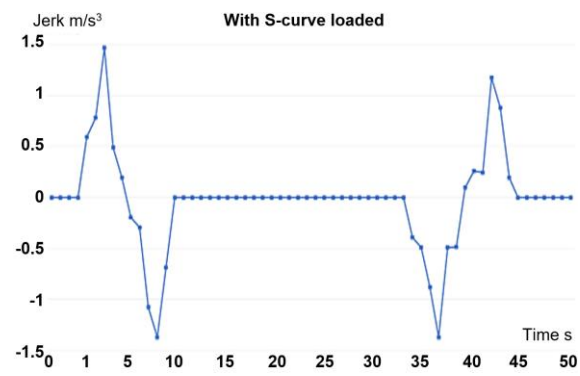


Figure 14. Jerk in the 4th case (with s-curve, loaded, downward)

Table 2. Comparison of control methods for elevator motion profiles

Feature	S-curve	Trapezoidal	Triangular	PID control
Jerk minimization	Excellent (smooth transitions)	Moderate (abrupt changes)	Low (sharp acceleration/deceleration)	Varies (depends on tuning)
Ride comfort	High (smoother acceleration)	Moderate	Low	Moderate
Acceleration/deceleration smoothness	Very smooth	Less smooth (step changes)	Abrupt	Dependent on tuning
Ease of implementation	Moderate (requires precise calculation)	Easy (simple shape)	Easy (linear shape)	Moderate to complex
Control complexity	Higher (more parameters to tune)	Lower	Lower	Moderate to high
Application in elevators	Ideal for passenger comfort	Suitable for simple applications	Rarely used due to abrupt motion	Commonly used with varying results

4.5. Interpreting the practical implications of jerk reduction

According to ISO 8100-34:2021, the maximum allowable jerk for elevators is 1.2 m/s³. In this study, the max jerk values ranged between 1.37 and 1.4 m/s³ under loaded conditions when using the S-curve profile, which, while slightly above the standard, marks a significant improvement over the conventional profile. The S-curves smoother acceleration offers a more stable ride, enhancing passenger comfort. With further

optimization and adjustments to the system, compliance with the ISO 8100-34:2021 limit could be achieved. This approach shows strong potential for improving elevator performance and reducing mechanical stress.

5. CONCLUSION

The implementation of the S-curve motion profile for the VFD using sensorless field-oriented control significantly reduces elevator jerk. The results indicate a jerk reduction of 29.43% to 48.78% under no-load conditions, and 48.15% to 52.08% under load conditions, with and without the S-curve, respectively. The difference in jerk profiles between loaded and unloaded conditions can be attributed to the impact of mass on the system's inertia. The increased mass in loaded conditions dampens abrupt acceleration changes, leading to smoother jerk transitions, while in no-load conditions, the system is more sensitive to acceleration changes. These findings underscore the effectiveness of the S-curve profile in minimizing jerk and ensuring smoother, safer elevator operation. The greatest improvements observed in loaded conditions highlight the S-curve's capability to enhance ride quality and reduce mechanical wear. Consequently, these results contribute to improved elevator efficiency, increased ride comfort, and reduced mechanical stress.

The findings highlight notable improvements but also reveal limitations and avenues for future research. Hardware constraints, such as the accelerometer's resolution, introduced noise into jerk measurements. The small-scale prototype lacked full-sized elevator dynamics like cable sway and building vibrations. Sensorless vector control also faced accuracy challenges under varying loads.

Future work could optimize S-curve parameters based on real-time loads for smoother performance. Exploring advanced methods like model predictive control (MPC) or AI-based algorithms could enable adaptive motion profile optimization. Full-scale tests on actual elevators would validate scalability and effectiveness. Integrating advanced sensors, such as load cells or high-resolution accelerometers, could improve real-time feedback and enable dynamic motion adjustments. Enhancing energy efficiency through optimized control algorithms, minimizing power use during acceleration and deceleration, and incorporating regenerative braking systems could further improve system performance.

FUNDING INFORMATION

This research received no specific funding from any funding agency in the public, commercial, or not-for-profit sectors.

AUTHOR CONTRIBUTIONS STATEMENT

This journal uses the Contributor Roles Taxonomy (CRediT) to recognize individual author contributions, reduce authorship disputes, and facilitate collaboration. All authors contributed equally to the conception, design, drafting, and revision of this manuscript. All authors have read and approved the final manuscript.

Name of Author	C	M	So	Va	Fo	I	R	D	O	E	Vi	Su	P	Fu
Ali Abdulkareem Ali	✓	✓							✓	✓				
Fatma Ben Salem	✓	✓							✓	✓				
Jamal A.-K. Mohammed	✓	✓							✓	✓				

C : **C**onceptualization

M : **M**ethodology

So : **S**oftware

Va : **V**alidation

Fo : **F**ormal analysis

I : **I**nterpretation

R : **R**esources

D : **D**ata Curation

O : Writing - **O**riginal Draft

E : Writing - Review & **E**dit

Vi : **V**isualization

Su : **S**upervision

P : **P**roject administration

Fu : **F**unding acquisition

CONFLICT OF INTEREST STATEMENT

Authors state no conflict of interest.

INFORMED CONSENT

We have obtained informed consent from all individuals included in this study.

ETHICAL APPROVAL

Ethical approval is not applicable to this paper, as the research did not involve human or animal subjects.

DATA AVAILABILITY

The authors confirm that the data supporting the findings of this study are available within the article and its supplementary materials.




REFERENCES

- [1] S. Feng, Y. Liang, J. Chen, and B. Chen, "Research on the change of traction force of elevator after decoration," *Journal of Physics: Conference Series*, vol. 2030, no. 1, 2021, doi: 10.1088/1742-6596/2030/1/012051.
- [2] P. Xu *et al.*, "Experimental study on damping characteristics of elevator traction system," *Advances in Mechanical Engineering*, vol. 14, no. 3, 2022, doi: 10.1177/16878132221085434.
- [3] G. Y. Kim and S. H. Jang, "Elevating innovation: Unveiling the twin traction method for a 50-ton load capacity elevator in building and construction applications," *Buildings*, vol. 14, no. 5, 2024, doi: 10.3390/buildings14051244.
- [4] J. A. K. Mohammed, W. Hashim, and B. Beram, "Performance improvement of a conventional hydraulic elevator by using electro-hydraulic servo mechanism," *Engineering and Technology Journal*, vol. 38, no. 5, pp. 748–760, 2020, doi: 10.30684/etj.v38i5a.367.
- [5] I. Abed Al-Hady, F. Mohammed, and J. A. K. Mohammed, "Modeling and simulation of telescopic hydraulic for elevating purposes," *Engineering and Technology Journal*, vol. 40, no. 1, pp. 226–232, 2022, doi: 10.30684/etj.v40i1.2253.
- [6] I. H. A. Al-Had, F. M. Mohammed, and J. A. K. Mohammed, "Modeling and simulation of electro-hydraulic telescopic elevator system controlled by programmable logic controller," *Indonesian Journal of Electrical Engineering and Computer Science*, vol. 27, no. 1, pp. 71–78, 2022, doi: 10.11591/ijeecs.v27.i1.pp71-78.
- [7] K. Izumi, H. Matsuoka, T. Mishiro, and H. Sano, "New style machine room-less elevator (elevator, escalator and amusement rides conference)," *The Proceedings of the Elevator, Escalator and Amusement Rides Conference*, vol. 2004, pp. 43–46, 2005, doi: 10.1299/jsmeearc.2004.43.
- [8] A. P. Nair, "A critical review and investigation of machine room less (MRL) elevators," *Journal of Applied Mechanical Engineering*, vol. 04, no. 03, 2015, doi: 10.4172/2168-9873.1000166.
- [9] J. S. Lee, B. S. Kim, and B. J. Jung, "Compacted governor design and analysis of machine room less type elevators," *Information (Japan)*, vol. 20, no. 5, pp. 3633–3640, 2017.
- [10] H. K. Kadhon and F. A.-K. Fattah, "Modification of electro - pneumatic elevator system depending on the air pressure and flow rate determinations," *Wasit Journal of Engineering Sciences*, vol. 6, no. 2, pp. 56–65, 2018, doi: 10.31185/ejuow.vol6.iss2.92.
- [11] K. Al-Kodmany, "Tall buildings and elevators: A review of recent technological advances," *Buildings*, vol. 5, no. 3, pp. 1070–1104, 2015, doi: 10.3390/buildings5031070.
- [12] M. A. Habibi, A. Wibawa, I. Fadlika, M. F. A. Irfani, M. F. Firmansyah, and A. Baskoro, "Study case on implementation elevator 2 floor system on PLC OMRON CP1E N30," *Proceedings - International Conference on Education and Technology, ICET*, pp. 158–163, 2023, doi: 10.1109/ICET59790.2023.10435313.
- [13] T. Dzhuguryan and Z. Józwiak, "Specific approach to select of freight elevators for multi-floor manufacturing," *AUTOBUSY – Technika, Eksploatacja, Systemy Transportowe*, vol. 19, no. 12, pp. 1059–1062, 2018, doi: 10.24136/atest.2018.550.
- [14] E. Ndembe and J. Bitzan, "Grain freight elevator consolidation, transportation demand, and the growth of shuttle facilities," *Research in Transportation Economics*, vol. 71, pp. 54–60, 2018, doi: 10.1016/j.retrec.2018.10.001.
- [15] D. M. Z. Islam and T. H. Zunder, "Experiences of rail intermodal freight transport for low-density high value (LDHV) goods in Europe," *European Transport Research Review*, vol. 10, no. 2, 2018, doi: 10.1186/s12544-018-0295-7.
- [16] R. Saidur, S. Mekhilef, M. B. Ali, A. Safari, and H. A. Mohammed, "Applications of variable speed drive (VSD) in electrical motors energy savings," *Renewable and Sustainable Energy Reviews*, vol. 16, no. 1, pp. 543–550, 2012, doi: 10.1016/j.rser.2011.08.020.
- [17] L. Al-Sharif, "Variable speed drives in lift systems," *Elevator World*, vol. 49, no. 9, pp. 96–104, 2001.
- [18] K. Ogudo and P. Umene, "Design of a transistor-based H-bridge DC motor drive circuit applied to an elevator for car doors transportation," *EasyChair Preprint 1704*, 2019.
- [19] D. Das, N. Kumaresan, V. Nayanar, K. N. Sam, and N. A. Gounden, "Development of BLDC motor-based elevator system suitable for DC microgrid," *IEEE/ASME Transactions on Mechatronics*, vol. 21, no. 3, pp. 1552–1560, 2016, doi: 10.1109/TMECH.2015.2506818.
- [20] A. S. Karthik, J. Batra, and S. S. Makadia, "Voice assistance goods lifter using rack and pinion," *International Journal of Electrical Engineering and Technology*, vol. 11, no. 7, pp. 17–24, 2020, doi: 10.34218/ijeet.11.7.2020.003.
- [21] Z. Li, Y. Ting, S. Tong, and H. Bao, "Research on load characteristics of rack and pinion drive system of shaft construction hoist," in *Sixth International Conference on Intelligent Computing, Communication, and Devices (ICCD 2023)*, S. Patnaik, Ed., SPIE, Jun. 2023, p. 27, doi: 10.1117/12.2682858.
- [22] P. G. Matthew, A. Kumar B, and P. A. Michael, "literature study and simulation of screw-type elevators," *Journal of Physics: Conference Series*, vol. 1362, no. 1, p. 012028, Nov. 2019, doi: 10.1088/1742-6596/1362/1/012028.
- [23] K. Kalpana, M. B. Reddy, S. Sailani, E. Poornima, and P. Chaudhary, "Design and fabrication of staircase elevator with lead screw mechanism for elderly people," *E3S Web of Conferences*, vol. 430, 2023, doi: 10.1051/e3sconf/202343001144.
- [24] W. D. Zhu and H. Ren, "A linear model of stationary elevator traveling and compensation cables," *Journal of Sound and Vibration*, vol. 332, no. 12, pp. 3086–3097, Jun. 2013, doi: 10.1016/j.jsv.2013.01.009.
- [25] A. Onat, E. Kazan, N. Takahashi, D. Miyagi, Y. Komatsu, and S. Markon, "Design and implementation of a linear motor for multicar elevators," *IEEE/ASME Transactions on Mechatronics*, vol. 15, no. 5, pp. 685–693, Oct. 2010, doi: 10.1109/TMECH.2009.2031815.
- [26] C. Li, C. Hua, J. Qin, and Z. Zhu, "Research on the dynamic characteristics of high-speed elevator system," in *Proceedings of the 2019 International Conference on Electronical, Mechanical and Materials Engineering (ICE2ME 2019)*, Paris, France: Atlantis Press, 2019, doi: 10.2991/ice2me-19.2019.23.




- [27] L. Qiu, Z. Wang, S. Zhang, L. Zhang, and J. Chen, "A vibration-related design parameter optimization method for high-speed elevator horizontal vibration reduction," *Shock and Vibration*, vol. 2020, pp. 1–20, Feb. 2020, doi: 10.1155/2020/1269170.
- [28] M. P. Shreelakshmi and V. Agarwal, "Jerk and loss minimization in electric elevator systems," in *2014 International Conference on Circuits, Systems, Communication and Information Technology Applications (CSCITA)*, IEEE, Apr. 2014, pp. 19–23. doi: 10.1109/CSCITA.2014.6839228.
- [29] I. Crăciun, M. Ungureanu, and A. Dăscălecu, "Considerations on the kinematics of an elevator with speed modeling and continuous deceleration," *Annals of the University of Petroșani, Mechanical Engineering*, vol. 17, pp. 27–34, 2015.
- [30] S. Masoudi, M. R. Feyzi, and M. B. B. Sharifian, "Force ripple and jerk minimisation in double sided linear switched reluctance motor used in elevator application," *IET Electric Power Applications*, vol. 10, no. 6, pp. 508–516, Jul. 2016, doi: 10.1049/iet-epa.2015.0555.
- [31] O. M. Arafa, M. E. Abdallah, and G. A. A. Aziz, "High-performance elevator traction using direct torque controlled induction motor drive," *Journal of Electrical Engineering and Technology*, vol. 13, no. 3, pp. 1156–1165, 2018, doi: 10.5370/JEET.2018.13.3.1156.
- [32] M. P. Shreelakshmi and V. Agarwal, "Trajectory optimization for loss minimization in induction motor fed elevator systems," *IEEE Transactions on Power Electronics*, vol. 33, no. 6, pp. 5160–5170, Jun. 2018, doi: 10.1109/TPEL.2017.2735905.
- [33] S. Rangarajan and V. Agarwal, "Load sensorless novel control scheme for minimizing the starting jerk and energy of the PMSM driven gearless elevators with varying stiction and rotor flux linkage," in *2019 IEEE Transportation Electrification Conference (ITEC-India)*, IEEE, Dec. 2019, pp. 1–6, doi: 10.1109/ITEC-India48457.2019.ITECINDIA2019-225.
- [34] M. K. Mutlu, "Limited-jerk sinusoidal trajectory design for field oriented control of permanent magnet synchronous motors with h-infinity optimal controller," *METU Thesis*, vol. 1, no. 1, pp. 1–13, 2019, [Online]. Available: <http://etd.lib.metu.edu.tr/upload/12624523/index.pdf>
- [35] A. A. Ali, F. B. Salem, and J. A.-K. Mohammed, "Enhancing elevator ride quality through vector control techniques and s-curve profiles," *Engineering, Technology & Applied Science Research*, vol. 14, no. 6, pp. 18785–18791, Dec. 2024, doi: 10.48084/etasr.9228.
- [36] A. Belbali, S. Makhoulfi, A. Kadri, L. Abdallah, and Z. Seddik, "Mathematical modeling of a three-phase induction motor," in *Induction Motors - Recent Advances, New Perspectives and Applications*, IntechOpen, 2023, doi: 10.5772/intechopen.1001587.
- [37] N. P. Quang and J. A. Dittrich, "Principles of vector orientation and vector orientated control structures for systems using three - phase AC machines," in *Power Systems*, vol. 20, 2015, pp. 3–16, doi: 10.1007/978-3-662-46915-6_1.
- [38] K. D. Nguyen, T.-C. Ng, and I.-M. Chen, "On algorithms for planning S-curve motion profiles," *International Journal of Advanced Robotic Systems*, vol. 5, no. 1, Mar. 2008, doi: 10.5772/5652.
- [39] A. A. Ali, F. Ben Salem, and J. A.-K. Mohammed, "Design of an electric elevator drive with high riding quality under jerk control," *Engineering, Technology & Applied Science Research*, vol. 14, no. 5, pp. 16438–16443, Oct. 2024, doi: 10.48084/etasr.8202.

BIOGRAPHIES OF AUTHORS






Ali Abdulkareem Ali    was born in Baghdad, Iraq, in 1990. He received the B.S. degree in 2012 and the Master's in 2016 from the University of Technology, Iraq. He is currently working toward Ph.D. in Electrical Engineering at Sfax Engineering School (SES), University of Sfax, Tunisia. His main research interests include electrical drives, power electronics, and elevators. He is a member of the research "CEMLab" laboratory of the SES. He can be contacted at email: ali-abulkareem.ali@enis.tn.



Fatma Ben Salem    was born in Sfax, Tunisia, in 1978. She received the B.S., the Master's, the Ph.D., and the HCR degrees in 2002, 2003, 2010, and 2015, respectively, all in electrical engineering from the National Engineering School of Sfax, University of Sfax, Tunisia. She is a professor of electrical engineering at the High Institute of Industrial Management of Sfax, Tunisia. She is a member of the Control and Energy Management Laboratory (CEMLab) of the University of Sfax. She is an IEEE member. Her main research interests cover several aspects related to the advanced control and the diagnostic of electric machine drives and generators involved in automotive, renewable energy systems, and smart grid technologies. She can be contacted at email: f.bensalem@psau.edu.sa.



Jamal A.-K. Mohammed    was born in Iraq. He obtained his B.Sc. of Electrical Engineering degree in 1996 and his M.Sc. of Electrical Engineering degree in 2002 from the University of Technology, Baghdad. His Ph.D. degree was awarded in 2007 by the University of Technology, Iraq, Baghdad. His research interests include electrical machines, electrical drives, power electronics, elevators, and renewable energy (solar). He has published close to 30 papers and has supervised several M.Sc. and Ph.D. theses. He can be contacted at email: 50128@uotechnology.edu.iq.